Journal of Spatial Hydrology
Vol.7, No.1, Spring 2007

Modeling hydrological response of the Upper Suriname river basin to climate change

R. Nurmohamed[1], S. Naipal[1], F. De Smedt[2]

Abstract

The goal of this paper is to assess the impact of future climate change on the hydrological regime of the tropical Upper Suriname river basin (7,860 km^2) located in Suriname. GCM based climate scenarios from the MAGICC/SCENGEN model and 14 hypothetical climate scenarios are used to examine potential changes in water balance components in the study area. A physically-based distributed hydrological model, WetSpa, and Geographic Information Systems (GIS) are used to simulate the historical and future hydrological conditions. The evaluation results indicate that the model has a relatively high confidence (model bias C1 is 0.046 and the model determinant coefficient C2 is 0.833) and can give a fair representation of the river flow hydrographs at daily scale (Nash Sutcliffe coefficient C3 is 0.622). The results indicate that an obvious increase in the annual temperature (1.8^{o}C and 3.2^{o}C by 2050 and 2080 respectively) in the study area is accompanied with a clear tendency in reduced precipitation during January-March and August-December, and an increased tendency during April-July. The sensitivity analyses of water balance components under temperature and precipitation change (GCM scenarios for 2050, 2080) shows that by 2080, the annual river discharge will drop 35%. The hypothetical climate scenarios (T+2^{o}C, T+4^{o}C and P$\pm$10%, $\pm$30%, $\pm$50%) however indicate that the annual river discharge will increase with maximum 75% for the scenario T+2^{o}C P+50% and will decrease with maximum 87.5% for the scenario T+2^{o}C P-50%. The results are indications of potential impacts of climate change on water resources in the Upper Suriname river basin, but true predictive skills require a significant improvement in the ability of global climate models to predictive changes in regional climate variability. The WetSpa model has proven to be useful for hydrological modeling studies where availability of physical catchment characteristics and hydroclimatic data is scarce.

Keywords: *C*limate Change; Climate Change Scenarios; Geographic Information Systems; Global Circulation Models; Hydrologic Modeling; Upper Suriname river basin.

Introduction

The increase in global mean surface air temperature by about 0.6°C $\pm$ 0.2°C over the late 20th century has affected the global hydrological cycle (Glen, 2004). According to climate models, the global surface temperature is likely to rise by about 1.5-3.5^{o}C by the end of 2100. A simple increase in temperature will increase evaporation and enable the atmosphere to transport higher amounts of water vapor. Therefore, it is assumed that rainfall and runoff will be accelerated. Long-term changes in precipitation on earth will affect water resources and, consequently different socio-economic sectors such as hydropower generation, drinking water supply, irrigation, ecosystems, forests and wetlands.

Predicting long-term climate change impacts on water resources using hydrological modeling and climate modeling is still a very intricate task. Currently, Global Circulation Models (GCMs)

[1] PhD student, [2] Associated Professor, Department of Infrastructure, Faculty of Technology, University of Suriname, Leysweg, POB 9212, Paramaribo, Suriname, [3] Professor, Department of Hydrology and Hydraulic Engineering, Vrije Universiteit Brussel, Pleinlaan 2, 1050 Brussels, Belgium
Corresponding author's email: r.nurmohamed@uvs.edu

are the most powerful climate models to predict changes in hydrometeorological variables (e.g. cloud cover, evaporation, temperature, precipitation, soil moisture) due to increasing levels of atmospheric greenhouse gases (Bronstert et al, 2002; Gleick, 1986; IPCC, 2001; IPCC-TGCIA, 1999). However, the outputs of the GCMs may not be used directly for climate impact analyses at basin scale due to the coarse resolution (about 300 km) and the fact that local climate (e.g precipitation) and/or hydrological processes are still not well reproduced in time and space by the GCMs. Therefore, the results of GCMs can only be used for sensitivity analyses. The use of hypothetical climate change scenarios can also be considered as an option to study future hydrological changes (Niemann et al 1994; Robock et al, 1993).

Hydrological models, using geographic information systems (GIS) techniques, are nowadays a powerful tool to understand current and future hydrological changes of a river basin (Boorman and Sefton, 1997; Gleick, 1986; Perrin et al, 2001). GIS techniques allow us to handle the spatial varied data in digital form and to derive basin parameters (e.g. slope, flow direction). There are a few classifications for hydrological models and they are somewhat arbitrary (Beven, 2000; Booij, 2002; Maidment 1992; Perrin et al 2001). In general, hydrological models can be classified in empirical, conceptual and physically based spatial distributed models. Some conceptual models are the Stanford watershed model (Crawford and Linsley, 1966), the HBV model (Bergstrom and Forsman, 1973) and the PRMS model (Leavesley et al, 1983). Some physically based spatial distributed models are the IHDM model (Calver and Woord, 1995), the TOPMODEL (Beven and Kirkby, 1979), the MIKE-SHE model (Refsgaard and Storm, 1995), the HBV model (Lindstrom et al, 1997) and the SWAT model (Arnold et al, 1998). The main differences between the first two and third group of models is that the empirical and conceptual models take no or very less account of the spatial distribution of physical data of the basin (e.g. soil, land use, topography) nor of the spatial variation of the climate (e.g. precipitation, evaporation), they have very few parameters to optimize, are easier to operate and require less data than the distributed models.

It has been shown that distributed hydrological models for (large tropical) catchments have important application to the prediction of the effect of climate change (Andersen et al, 2001; Bormann, 2005; Campling et al, 2002; Gleick, 1986; Roulin, 1998; Legesse et al, 2003; Liu, 1999; 2004; Menzel and Burger, 2002; Molicova et al, 1997; Perrin et al, 2001). For example, Legesse et al (2003) applied a physical distributed precipitation-runoff model, PRMS, to the Ketar river basin (3,220 km^2) in Ethiopia and arbitrary climate scenarios. This study shows that a 10% change in daily rainfall results in a decrease in annual runoff of about 30%. The model has shown to produce relative good results for an area with poor data. The main conclusions from many of the above case studies is that the predicted climate change impacts are influenced by the model performance and the lack of spatial detail in GCMs, which makes it difficult to reflect the inhomogeneous spatial pattern in precipitation and evapotranspiration. The model performance is mainly influenced by the inadequacy of the model structure, errors in data, the lack of high resolution topographic, soil and land use maps, the lack of sufficient rainfall stations and measurements of potential evapotranspiration, and information on soil hydraulic processes.

In the tropical part of South America, the climate is mainly characterized by a large inter annual to decadal variability in rainfall and river discharges caused by the variability in sea surface temperature (Ambrizzi et al, 2005; Giannini et al, 2000; Marshall et al, 2001; Martis et al, 2002; Rajagopolan et al, 1997; Wang, 2001, 2005). In Suriname (2^o-6^o Northern Length, 54^o-58^o Western Length), the sensitivity to short term climatic fluctuations can be illustrated by

prolonged dry (drought) and wet periods (heavy rainfall, floods). Some prolonged dry periods were in (a) north-west Suriname during 1925-1926, 1939-1940, August-November 1982, December 1982-February 1983, August 1997-February 1998, and (b) in central Suriname (Houben and Molenaar, undated; Mol et al, 2000). Some floods were experienced in (a) south-west and central Suriname during the first half of 2000, April 2004, and (b) northern Suriname (Paramaribo) during September 2004, July-August 2005 (Hollande, N., personal communication, October 1, 2004; Scheltz, E., personal communication, September 5, 2004).

One of the sensitive areas in Suriname is the Upper Suriname river basin (Fig. 1), which is the main source of water for the Prof. Dr. Ir. van Blommenstein reservoir. This artificial reservoir is being used for hydropower generation (189 Megawatts) for industrial and domestic purposes, and is therefore very important for the economy of Suriname. This reservoir has also been affected by prolonged dry periods such as in 1987-1988 (18 months), March 1999, January 2001 and September 2004-January 2005. The continuing increase in global temperature on earth (IPCC, 2001), makes it necessary also to understand how river flows and/or water balances of river basins my change due to long term climate changes as it will impact the management of water resources. The goal of this paper is therefore to understand how water resources in the Upper Suriname river basin (Suriname) might change due to future climate change by using a hydrological model and climate change scenarios.

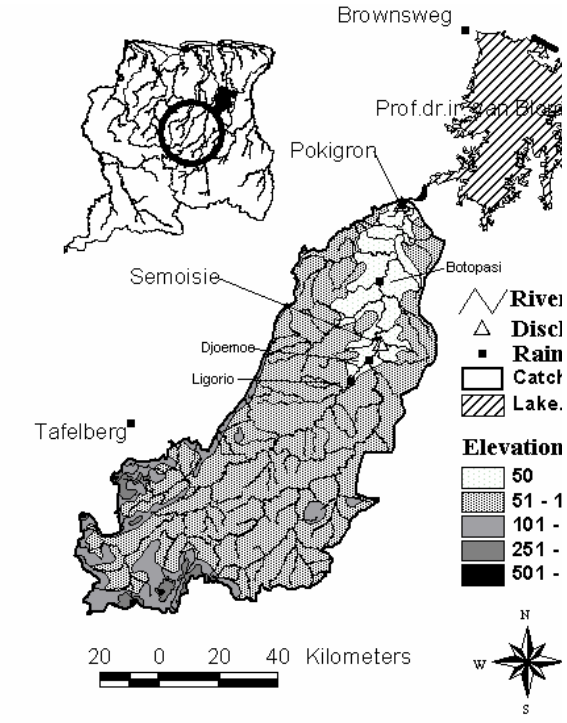

Figure 1: Location map of the Upper Suriname river basin (Suriname) and measuring networks.

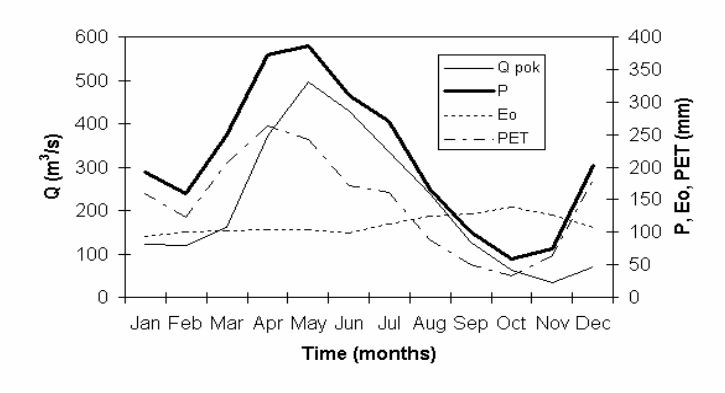

Figure 2: Mean monthly precipitation (P), pan evaporation (Eo), potential evapotranspiration (PET) and river discharge (Q_{pok}) in the Upper Suriname River basin.

Study area and data used

Selected catchment

The Upper Suriname River basin is situated in Suriname and has a total drainage area iof about 7,860 km^2 up till Pokigron (Fig. 1). The topography varies from 75 m to 809 m above mean sea level. The natural vegetation comprises high tropical dense forest. The different soil types in this basin are: sand (1.6%), silt (5.5%), silt clay loam (48.2%), clay loam (27.9%) and clay (16.8%). Till today, no significant changes in land use have been observed in this area. The basin is characterized by a tropical humid climate with a substantial seasonal variation. Fig. 2 shows plots of the mean monthly values of precipitation, estimated pan evaporation, stimated potential evapotranspiration and river discharge in the basin. These values are arithmetic mean of the variables of the stations, as shown in Fig. 1. The highest average precipitation is observed in May and is about 386 mm and the lowest average precipitation is observed in October and is about 58 mm (Nurmohamed and Naipal, 2004). The monthly pan evaporation in the study area varies from 93 mm in January to 138 mm in October (Lenselink and van der Weert, 1970). The highest discharge is reached in June and is about 495 m^3/s and the lowest discharge is about 34 m^3/s in November. The annual precipitation in this area is about 2,300 mm for the lower part of the basin and increases to 2,800 mm for the upper part of the basin. The annual pan evaporation is around 1,850 mm. The annual discharge at Pokigron (1952-1985) is about 219 m^3/s.

Data collection

Daily and monthly series of six rainfall stations (1961-1983) in or close to the study area (station Brownsweg, Pokigron, Botopasi, Djoemoe, Ligorio and Tafelberg) were obtained from the Meteorological Service Suriname. Records of mean daily river discharge (1952-1985) at two stations (Pokigron and Semoisie) were obtained from the Hydraulic Research Division Suriname and the Bureau for Hydroelectric Power Works. Only these stations were found suitable for use in this study in terms of data length and continuity. The network of these stations is shown in Fig. 1. Pan evaporation (Eo) data is very scarce in this area. Therefore, pan evaporation data (1975-1983) at Pokigron has been interpolated from station Coeroeni (at about 233 km) and Sipaliwini (at about 216 km) and pan evaporation data at Semoisie has been interpolated from station Stoelmanseiland (at about 120 km). Although these stations are very far, they are the closest stations to the study area with mostly complete daily bserved data. The actual evapotranspiration (ET) is estimated from the long-term water balance in this

basin, ET = Q-P, with ET = k*Eo, where Q is the river discharge, P is the precipitation, Eo is the pan evaporation, k is a monthly factor. The years 1975-1983 were finally selected because they have sufficient daily data to use for hydrological modeling purposes.

To complete missing data of precipitation and discharge, linear interpolating is done. The linear correlation coefficient (Pearson) between the monthly rainfall data of the stations ranges from 0.51 to 0.82. The river flows at Semoisie and Pokigron show a high consistency with a cross correlation coefficient of 0.95 for lag 0 and 0.71 for lag 1 month. A topographic map with river network of 1:100,000 (50 m interval) from year 1963, a soil map of 1:100,000 from 1963 and a land use map of 1:100,000 from 1963 were obtained from the Center of Natural Resources and Assessment (Narena). Observed baseline precipitation and temperature data used in the GCMs were taken from the Climatic Research Unit global 0.5 x 0.5^{o} 1961-1990 climate archive.

Methodology

In this paragraph, the WetSpa model is first described, followed by the way the input data has been processed. In the last section, an explanation is given on how the different climate change scenarios have been constructed.

Description of the WetSpa model

WetSpa is a continuous, distributed, physically-based hydrological model with variable time step (hourly or daily). This model is developed by the Vrije Universiteit Brussel, Belgium (Liu and De Smedt 2004) and has been applied to small and medium catchments (34-1,176 km^2) in Belgium, Luxembourg, Slovakia and Hungary. Liu et al (1999, 2004) and Seifu (2003) have shown that the model is suitable for simulation of spatial distribution of hydrological processes and analysis of land use changes and climate change impacts of hydrological processes. The model structure is shown in Fig. 3 and the hydrological processes are summarized in Table 1.

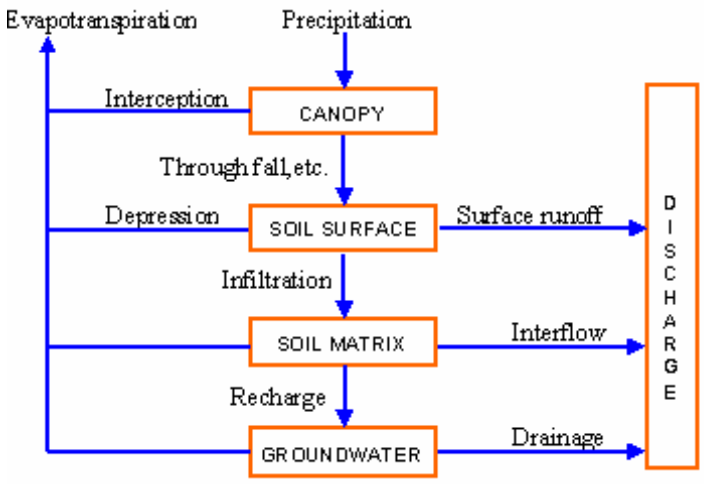

Figure 3: Schematic representation of the different components of the WetSpa model at a pixel cell level (Liu and De Smedt, 2004)

Table 1: Main hydrological processes and components per grid cell and equations of the WetSpa model (Liu, 2004)

Process	Equation	Approach
Basin water balance	P = RT+ET+ΔSS+ΔSG	-
Precipitation P	$P = \sum_{t=0}^{T} \sum_{i=1}^{N_w} P_i(t) / N_w$ (mm)	-
Total runoff RT	$RT = \sum_{t=0}^{T} \sum_{i=1}^{N_w} \left[RS_i(t) + RI_i(t)\right] / N_w + \sum_{t=0}^{T} \sum_{s=1}^{N_r} \frac{QG_s(t)}{A_s} / N_w$ (mm)	-
Overland flow RSi	$RS_i(t) = PE_i(t)\left[1 - \exp\left(-\frac{PE_i}{SD_{i,0}}\right)\right]$ (mm)	Linear diffusive wave approximation (Miler and Cunge, 1975)
Interflow or subsurface runoff RIi	$RI_i(t) = \frac{c_s D_i S_i K\left[\theta_i(t)\right]\Delta t}{W_i}$ (mm)	Darcy's Law and kinematic approximation
Groundwater outflow QGs(t)	$QG_s(t) = Kg\left[SG_s(t)/1000\right]^2$ (mm)	Non-linear reservoir method (Wittenberg and Sivapalan, 1999)
Groundwater balance SGs(t)	$SG_s(t) = SG_s(t-1) + \frac{\sum_{i=1}^{N_s}\left(RG_i(t)\right)A_i}{A_s} - EG_s(t) - \frac{QG_s(t)\Delta t}{1000 A_s}$ (mm)	-
Percolation RGi	$RG_i(t) = K_i(\theta_i(t))\Delta t = K_{i,s}\left(\frac{\theta_i(t) - \theta_{i,r}}{\theta_{i,s} - \theta_{i,r}}\right)^{(2+3B)/B} \Delta t$ (mm)	Darcy's law and Brooks and Corey relationship (Brooks and Corey, 1966; Eagleson, 1978)
Evapotranspiration ET	$ET = \sum_{t=0}^{T} \sum_{i=1}^{N_w} \left[EI_i(t) + ED_i(t) + ES_i(t)\right] / N_w + \sum_{t=0}^{T} \sum_{s=1}^{N_r} EG_i(t) / N_w$ (mm)	-
Change in soil moisture ΔSS	$\Delta SS = \sum_{t=1}^{N_w} D_i\left[\theta_i(T) - \theta_i(0)\right] / N_w$ (mm)	-
Change in groundwater storage ΔSG	$\Delta SG = \sum_{s=1}^{N_w}\left[SG_s(T) - SG_s(0)\right] / N_r$ (mm)	-

Abbreviations: T is the simulation period (s), N_w is the number of cells over the basin, $RI_i(t)$ is interflow out of a cell over time interval Δt (day) (mm), c_s is a scaling parameter, D_i is the root depth (mm), S_i is the cell slope (m/m), $K(\theta_i)t$ is the effective hydraulic conductivity (mm/hour), W is the cell width (mm), Kg is the non-linear groundwater flow recession

coefficient (m/s), $SG_s(t)$ groundwater storage of a subcatchment at time t (mm), c_v is the vegetation coefficient, $\theta_{i,f}$ is the soil moisture content at field capacity (m^3/m^3), $\theta_{i,w}$ is the soil moisture content at plant wilting point (m^3/m^3), $ES_i(t)$ is the actual evaoptranspiration (mm), EDi(t) is cell evaporation (mm), EP is the daily potential evaporation (mm), EI_i (t) is the evaporation from the cell interception storage (mm), t is the time step, A_i is the cell area (m^2), A_s is the sub basin area (m^2), $QG_s(t)$ is the groundwater discharge (m^3/s), EG_i (t) is the average evapotranspiration from groundwater storage of the sub basin (mm), c_r is the runoff coefficient, θ is the soil moisture content (m^3/m^3), θ_s is the soil porosity (m^3/m^3), K_s is the saturated hydraulic conductivity, θ_r is the residual soil moisture content (m^3/m^3), B is the cell pore size distribution index, Nr is the number of subcatchments, $\theta_i(T)$ and $\theta_i(0)$ is the cell soil moisture constant at time T and time 0 (m^3/m^3).

The main input data in the WetSpa model are digital spatial data (elevation, river network, land use and soil type), and hydrological and weather data (precipitation, evapotranspiration, discharges). For calibration of the model, nine global input parameters (Table 2) can be used for tropical areas. Most of the parameters are found through calibration. The main outputs of the WetSpa model are river flow hydrographs for the entire basin and subbasins (e.g. surface runoff, interflow, groundwater flow), water balance and spatial distributed hydrological characteristics for the entire basin at each time step (e.g. runoff, soil moisture, groundwater recharge, infiltration rates) (Liu et al, 2004; Seifu 2003).

Table 2: Global input parameters in WetSpa (Liu, 2004)

Parameter	Name	Unit	Range (best value)	Method of estimation
ki	interflow scaling factor	-	1-10	ratio of horizontal and vertical hydraulic conductivity; calibration recession curve observed and computed hydrograph
Kg	groundwater flow recession coefficient	-	< 0.01 or ki	calibration of observed and computed low flow hydrographs
K_ss	initial soil moisture	mm	-	calibration
go	initial groundwater storage in depth	mm	-	calibration of observed and computed low flows for initial phase
G_max	maximum groundwater storage in depth	mm	-	calibration
K_ep	correction factor for potential evapotranspiration	-	~ 1.0	calibration of water balance simulation
K_run	the surface runoff exponent	-	1-3	calibration
P_max	maximum rainfall intensity	mm/day	-	from observations observations

Table 3: Evaluation criteria for the model performance

Criteria	Description	Range (best value)	Source
$C1 = \frac{\sum_{i=1}^{N} Qs_i - Qo_i}{\sum_{i=1}^{N} Qo_i}$	Model bias for evaluating the ability to reproduce water balance	0	Liu, 2004
$C2 = \frac{\sum_{i=1}^{N} \left(Qs_i - \overline{Qo}\right)^2}{\sum_{i=1}^{N} \left(Qo_i - \overline{Qo}\right)^2}$	Determinant coefficient representing the simulation variance (model confidence)	0-1 (1)	Liu, 2004
$C3 = 1 - \frac{\sum_{i=1}^{N} \left(Qs_i - Qo_i\right)^2}{\sum_{i=1}^{N} \left(Qo_i - \overline{Qo}\right)^2}$			
$C4 = 1 - \frac{\sum_{i=1}^{N} [\ln Qs_i - \ln Qo_i]^2}{\sum_{i=1}^{N} [\ln Qo_i - \ln \overline{Qo}]^2}$	Model efficiency for evaluating the ability of reproducing river flows	< 1 (1)	Nash and Sutcliffe, 1970
$C5 = 1 - \frac{\sum_{i=1}^{N} (Qs_i + \overline{Qo})(Qs_i - Qo_i)^2}{\sum_{i=1}^{N} (Qo_i + \overline{Qo})(Qo_i - \overline{Qo})^2}$	Model efficiency for evaluating the ability of reproducing low flows	< 1 (1)	Smatkhin et al, 1998
	Model efficiency for evaluating the ability of reproducing high flows	< 1 (1)	Guex, 2001; USACE, 1998

Abbreviations: Qs_i is the simulated river flow at time step i (m^3/s), Qo_i is the observed river flow at time step i (m^3/s), N is the number of time steps, $\overline{Qo}$ is the mean observed river flows.

The calibration period (January 1978 to December 1981) and the validation period (January 1982 to December 1983) are selected for modeling analyses with a model initialization period set to 1975-1977. To determine how well the observed hydrographs are reproduced by the model, five model efficiencies (C1, C2, C3, C4, C5) are used (Table 3) and a visual inspection of the joint plots of the daily/monthly simulated and observed hydrographs is used to judge the ability of the model to simulate seasonal variability and extreme conditions. The global input parameters are adjusted till a satisfactory performance of the model is obtained.

Data processing

From the topographic contour map, a 10 m elevation contour map with grid size 50 m (slope factor 0.5, threshold factor 1.0) was first created from a 50 m elevation contour map using the ArcView Contour Gridder extension. Different resolution digital elevation models (DEM) were created (50 m, 100 m, 200 m, 500 m) using the TOPOGRID function in Arc/Info. From visual

comparison of the actual river network and the generated river network and because of computation time and computer memory, the 100 m DEM was accepted for further model simulation. From the DEM, the following physical parameters for each grid cell were created by ArcView: stream orders and network, slope of overland flow and river channels, flow direction, flow accumulation, subwatersheds based on stream links and the hydraulic radius according to a flood frequency of 2 years.

The soil information was first reclassified according to the 12 U.S. Department of Agriculture soil texture classes (USDA) used in WetSpa and then also converted to a 100 m grid map. From the soil map, different maps of physical properties such as porosity, hydraulic conductivity, residual moisture, pore index field capacity, wilting point were created using the default parameters characterizing the soil of the study area (Table 4). The land use information was also converted into six land use classes used in WetSpa and then also converted to a 100 m grid. From this map, different maps of physical properties are calculated such as root depth, Manning's coefficient and interception capacity using the default parameters characterizing the land use of the study area (Table 5). Based on the combination of DEM, soil and land use map, the potential runoff coefficient and depression capacity maps were created. The flow routing parameters are calculated using ArcView GIS using the slope, hydraulic radius and manning coefficient maps. From the results we can conclude that the average potential runoff coefficient is mainly between 0.2 and 0.4, while in the mountainous area values of up to 0.7 are reached. This is due to the steeper slopes in the mountainous area. The point rainfall data of six stations are used to create areal rainfall distribution, using the ArcView Thiessen polygon extension. For potential evapotranspiration, a Thiessen polygon map is also created based on time series at two locations.

Table 4: Default parameters characterizing the soil in the study area (Liu and de Smedt, 2004)

Texture class	Hydraulic conductivity (mm/h)	Porosity (m^3/m^3)	Field capacity (m^3/m^3)	Wilting point (m^3/m^3)	Residual moisture (m^3/m^3)	Pore size distribution index
Clay loam	1.51	0.464	0.310	0.187	0.075	8.32
Sand	208.80	0.437	0.062	0.024	0.020	3.39
Silt clay loam	4.32	0.398	0.244	0.136	0.068	7.20
Clay	0.60	0.475	0.378	0.251	0.090	12.13
Silt	6.84	0.482	0.258	0.126	0.015	3.71

Table 5: Default parameters characterizing the land use in the study area (Liu and de Smedt, 2004)

Land use class	Vegetated fraction (%)	Leaf area index	Root depth (m)	Manning's coefficient ($m^{-1/3}$ s)	Interception capacity (mm)
Evergreen broad leaf tree	90	5-6	1.5	0.60	0.15-2.00
Tall grass	80	0.5-6.0	1.0	0.40	0.10-1.50

The WetSpa model is finally run using observed daily rainfall, potential evapotranspiration and the derived physical parameters from digital elevation, land use and soil maps in ArcView GIS for both the semi-distributed and fully distributed model. In WetSpa, the fully distributed model

operates on cell scale and a variable time step and the semi-distributed model on small subwatershed scale.

Climate change scenarios

The MAGICC/SCENGEN climate model has been the primary model used by the Intergovernmental Panel on Climate Change (IPCC) and is therefore also used in this study to develop GCM based climate change scenarios. The following GCMs have been selected for this study: Had300 (UK Hadley Centre for Climate Prediction and Research, Europe), ECH498 (German Climate Research Centre, Germany), GFDL90 (US Geophysical Fluid Dynamics Laboratory, USA), CSI296 (Commonwealth Scientific and Ind. Research Organization, Australia) and CCSR96 (Japanese Centre for Climate Systems Research, Japan) (Assessed June 5, 2005 from http://www.pcmdi.llnl.gov/projects/cmip/overview_ms/table1.html and http://www.grida.no/climate/ipcc_tar/wg1/316.htm#tab81). A study by Nurmohamed and Naipal (2004) has shown that the GCMs, although with a spatial resolution of 550 km, represent the seasonal variation in temperature and precipitation in Suriname reasonably well. The GCMs are used to simulate the average monthly change in temperature and precipitation for two time frames 2035-2064 (2050) and 2065-2094 (2080). The daily change is calculated by dividing the monthly change by 30 days. The daily temperature and precipitation changes for year 2050 and 2080 have been added to the 9 years of daily observed data (1975-1983) (IPCC-TGCIA, 1999; Hulme et al, 2000; Wigley, 2003). These future data time series are used as inputs in the WetSpa model to simulate future changes in water resources in the study area. The average of the outputs of the GCMs is used to present climate change for the study area, rather than outputs of a single GCM (Hulme et al, 2000). We will assume that the spatial and temporal pattern is constant, but only the magnitude will change. We should however remark that the periods of the observed data series in the study area (1975-1983) and the period of the baseline GCM data series (temperature: 1961-1990; precipitation: 1981-2000) are different.

Because of the already mentioned limitations of GCMs (see paragraph 1), we will also use hypothetical scenarios. This method is adopted from Gellens and Roulin (1998) and is widely used. Changes in temperature of +2^{o}C and +4^{o}C and/or precipitation changes of $\pm$10%, $\pm$30% and $\pm$50% are adopted as scenarios. Such kind of scenarios have also been used by Booij, 2002, 2005; Boorman et al, 1997; Bormann, 2005 and Bronstert et al, 2002. Compared to the GCM scenarios, the changes are here applied uniformly to the entire historical daily data series in the study area: future temperature data time series are created by adding to each historical daily observed temperature value, a change of +2^{o}C or +4^{o}C, and future precipitation data time series are created by adding to each historical daily observed precipitation value, a change of $\pm$10% or $\pm$30% or $\pm$50%. Based on a linear relationship between the observed actual evaporation and the observed temperature in the study area, the future evapotranspiration is estimated using the future temperature (Wigley, 2003). The future change in temperature is used to estimate the future change in evapotranspiration. It is simple assumed that evaporation changes linearly with temperature (Wigley, 2003). The WetSpa model is finally set up to run the GCM scenario years 2050 and 2080 and a total of 14 hypothetical scenarios. Precipitation and evapotranspiration data for the period 1975-1983 represent current climate conditions (1xCO_2 concentration), and the GCM and hypothetical scenarios represent climate change conditions (2xCO_2 concentration).

Results and analyses

Calibration and validation results of the WetSpa model

A manual calibration is used, starting with a first estimation of ki, Kg, K_ss, K_ep, go and G_max, using the methods and/or ranges mentioned in Table 2. The model is re-runned (about 75 runs) to obtain a good match between the observed and simulated river flow hydrographs. The judgment is based on numerical evaluation of the results. The following optimum global parameters were found and are used for further analyses : ki = 1.0, Kg = 0.01, K_ss = 1.0, K_ep = 1.0, go = 30 mm, G_max = 400 mm, K_run = 1.5, P_max = 300 mm/day. It was shown that the model performance is mainly affected by the global input parameters (the interflow scaling factor, the groundwater flow recession coefficient, the initial soil moisture and the initial groundwater storage).

Table 6: Model performance for the calibration/validation period (1975-1983) for the Upper Suriname River basin at station Pokigron. C1 to C5 are the model evaluation criteria.

Model	**Model evaluation**				
Semi-distributed model	***C1***	***C2***	***C3***	***C4***	***C5***
Calibration (1978-1981)	-0.011	0.839	0.543	0.555	0.643
Validation (1982-1983)	0.194	0.875	0.768	0.633	0.850
Total (1978-1983)	0.046	0.833	0.622	0.609	0.715
Fully distributed model					
Calibration (1978-1981)	-0.219	0.726	0.552	0.493	0.585
Validation (1982-1983)	-0.029	0.794	0.779	0.779	0.804
Total (1978-1983)	-0.166	0.727	0.631	0.659	0.662

Table 6 shows the comparison in model evaluation criteria for the semi-distributed and fully distributed model. It is found that the most sensitive global input parameters are ki, Kg, K_ss and go. From the results, we can also see that the semi-distributed model produces slightly better evaluation results than the fully distributed model. The calibration and validation results show that there is a reasonably moderate agreement between the measured and simulated river flows during this period. WetSpa reproduces the observed water balance (1978-1983) with 4.6% overestimation, the Nash-Sutcliffe model efficiency for reproducing the river flows is about 62% and the ability to reproduce low and high flows is 62% and 71% respectively. The model confidence is 83%. Figure 4 shows a typical calibration result for year 1982 corresponding to the chosen global input parameters. From this result we can clearly see that the model has simulated the seasonal and inter-annual variability in river discharge in the basin very well. The increase in river flow can be explained by the heavy rainfall events and the increase in base flow (interflow and groundwater flow) during January - mid-June. The decrease in flow after mid-June can be explained by the decrease in rainfall events and the base flow.

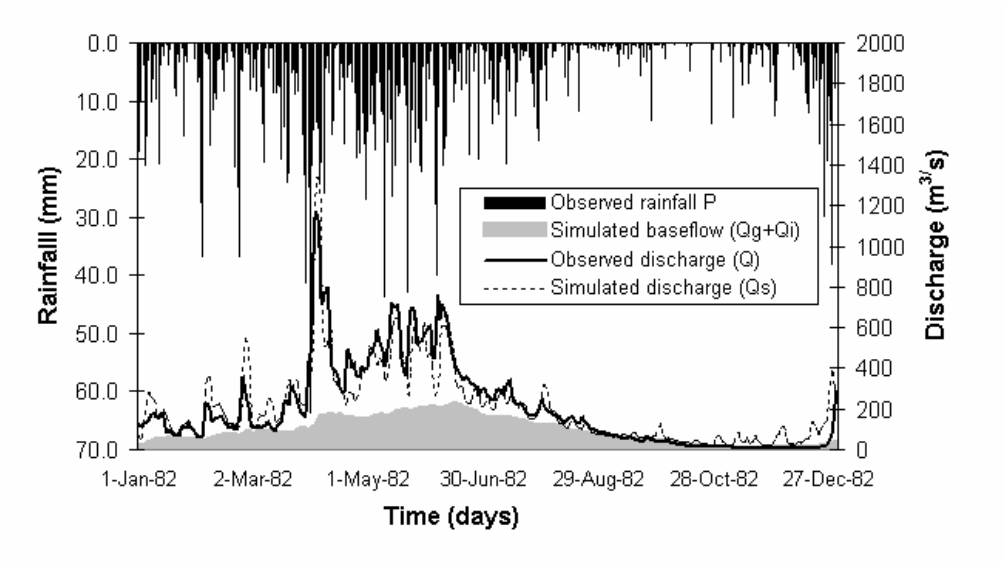

Figure 4: Mean daily observed and simulated river discharge and simulated base flow at Pokigron for 1982 (semi-distributed model).

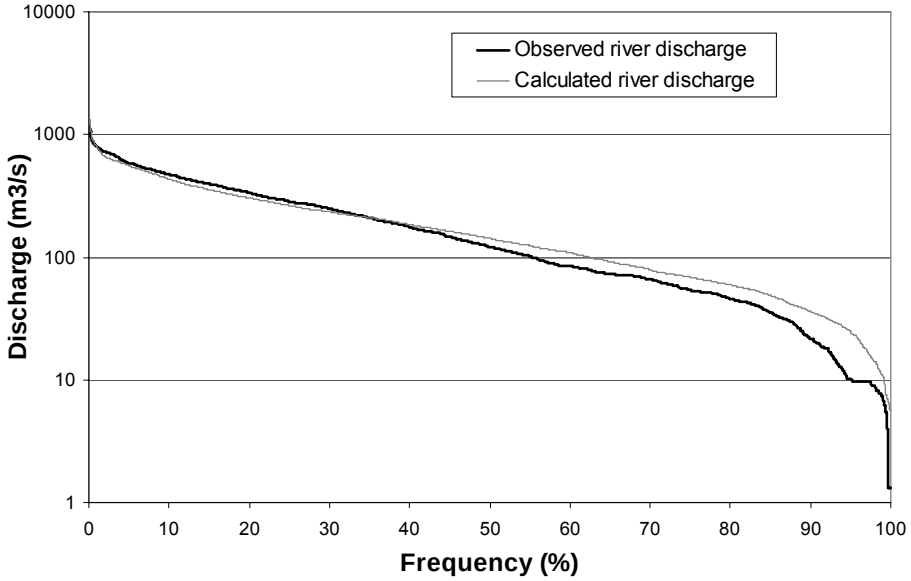

Figure 5: Comparison of the ranked value of the daily observed and simulated mean flows at Pokigron (1978-1983)

Analyses of the ranked value of the observed and simulated flows indicates that there are some obvious deviations for low flows (Q < 160 m^3/s) and for high flows (Q > 220 m^3/s) (Fig. 5). The error for small flows is up to 436%, especially for flows smaller than 30 m^3/s and for large flows up to 23%. The large errors for small flows are caused by lack of observations, especially during the dry seasons (September-November). The errors for large flows may be caused by the use of daily observations, which cannot accurately capture storm events causing floods. The shortness of the data series may also have affected the calibration results. The lack of other measurements of the hydrological processes (e.g. groundwater flow,

infiltration) makes it also difficult to estimate the base flow recession coefficient, the surface runoff coefficient and the maximum groundwater storage and may also contribute to the large errors in low flows and high flows respectively. The deviations between the observed and simulated flows may further also be caused by the lack of a good representation of the meteorological conditions in the study area. The spatialization of point rainfall and evaporation data may also affect the quality of the hydrological simulation. Rainfall and evaporation stations are very scarce and the stations are generally located along the river. Other reasons are deficiency of model structure (Liu, 2004), low resolution and errors in the elevation, soil and land use maps, and the default input parameters used in the model.

Table 7: Observed and simulated water balance of the Upper Suriname river basin for the period 1978-1983.

Component	**Observed (mm)**	**Percentage of P (%)**	**Simulated (mm)**	**Percentage of P (%)**
Precipitation	14173	**100**	14052	**100**
Interception			1162	8.3
Infiltration			9453	67.3
Actual evapotranspiration	9237	**65.2**	8528	**60.7**
Percolation			5053	35.9
Surface runoff			2667	19.1
Interflow			112	0.8
Groundwater flow			2177	13.9
Total runoff	4736	**33.4**	4956	**35.3**
Soil moisture difference			-28	-0.2
Groundwater storage			-51	-0.3

Table 7 summarizes the observed and simulated water balance for the period 1978-1983. It is evident that, the observed and simulated precipitation and total runoff water balance components do not differ much from each other. The simulated water balance shows that the total runoff of the Upper Suriname River basin is composed of 57% surface runoff and 43% base flow (groundwater flow and interflow). The seasonal water balance analyses show that when the river discharge increases in the Upper Suriname river during December-February and March-May (wet season), the amount of surface runoff is about 60% and base flow about 40% of the total runoff and does not change significantly during both periods (see Fig. 4).

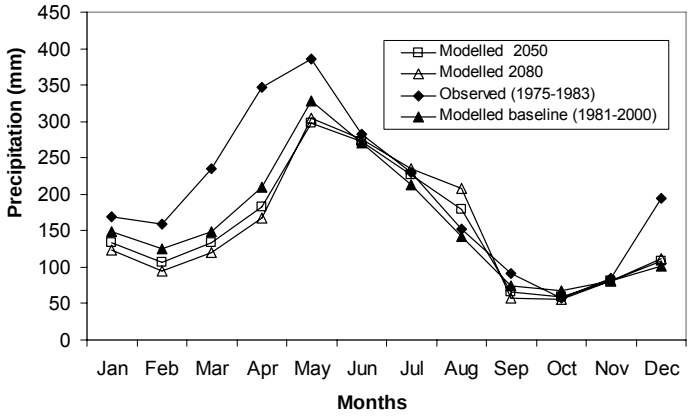

Figure 6: Observed precipitation (1975-1983) in the Upper Suriname river basin, modeled observed baseline precipitation (1981-2000) and simulated future precipitation (2050, 2080) predicted by GCMs climate scenarios.

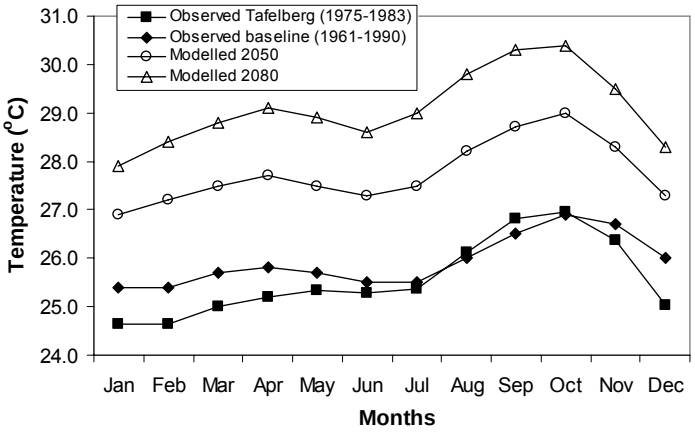

Figure 7: Observed temperature (1973-1985) near the Upper Suriname river basin (station Tafelberg), modeled observed baseline temperature (1961-1990) and simulated future temperature (2050, 2080) predicted by GCMs climate scenarios.

When the discharge decreases, base flow dominates during June-August and September-November (long dry season) and is about 67% and 74% of the total runoff respectively. Surface runoff is about 33% and 26% of the total runoff during June-August and September-November respectively. It is also concluded from the results that, during the low flow period, the model evaluation results are the lowest.

Climate change scenarios simulation

Figure 6 shows the mean observed precipitation (1975-1983) and the modeled baseline precipitation (1981-2000) for the current climate, and the future monthly precipitation from the GCM outputs (2050, 2080) for the study area. The Pearson's correlation coefficient (r) between the observed and modeled baseline monthly time series is 0.91 ($p < 0.05$), from which we can conclude that the GCM follows the seasonal pattern well. Two 30-year periods, namely 2035-2065 (2050) and 2070-2099 (2080) are used to estimate the future climate. The observed annual precipitation (1978-1983) in the study area is 2,388 mm and the modeled annual baseline precipitation (1981-2000) is 1,915 mm. This is a difference of about 20%.

The GCMs predict a decrease in precipitation during January-May with a maximum difference of 31.0 mm/month (8%) during May and a decrease of about 9 mm/month during September-October. By 2050, an increase is predicted during June-August with a maximum difference of 37.2 mm/month (24.2%) in August and 6.2 mm/month in December. The same pattern is found for 2080 but with higher values: a decrease in precipitation during January-May with a maximum difference of 43.4 mm/month (12.6%) in April and a decrease of about 12.4-18.6 mm/month during September-October. During June-August, precipitation is expected to increase with a maximum difference of 65.1 mm/month (42.5%) in August and 9.3 mm/month in December. The annual precipitation in the basin will slightly decrease with about 68 mm (2.8%) in 2050 and 78.6 mm (3.3%) in 2080.

Figure 7 shows the mean observed temperature (1975-1983) for station Tafelberg and the modeled baseline temperature (1961-1990) from the five GCMs for the study area. The seasonal pattern of monthly temperature is also well simulated by the GCMs ($r = 0.90$; $p < 0.05$). The observed annual temperature (1978-1983) in the study area is 25.6^{o}C and the modeled annual baseline temperature (1961-1990) is 25.9^{o}C. This is a difference of 0.3°C. The annual temperature in the study area is predicted to increase with 1.8^{o}C and 3.2^{o}C by 2050 and 2080 respectively. Figure 7 also shows the predicted mean monthly temperature corresponding the years 2050 and 2080. The GCMs predict an increase in mean temperature during all the months with a maximum of 2.2^{o}C in September/October by 2050 and 3.8^{o}C in September/October by 2080.

From the predicted changes in temperature (Fig. 7), the future changes in pan evaporation are calculated. The annual pan evaporation in the study area is estimated to increase with about 1,048 mm (78%) by 2080 (if temperature increases 3.2^{o}C). The historical monthly temperature series from the GCMs and the evaporation series at Pokigron and Semoisie have a correlation coefficient of 0.92 ($p < 0.05$) and 0.87 ($p < 0.05$) respectively. Fig. 8 shows the mean observed evaporation in the study area and the mean evaporation for 2050 and 2080. The highest increase in evaporation is estimated to be in September and is 2.6 and 4.3 mm/day by 2050 and 2080 respectively. Evapotranspiration is calculated according to the procedure mentioned in paragraph 3.3. The actual annual evapotranspiration in the study area is predicted to increase with 643 mm (8%) and 1401 mm (17%) by 2050 and 2080 respectively. The changes in evapotranspiration are in the same order of magnitude as reported by Verhoog (1987).

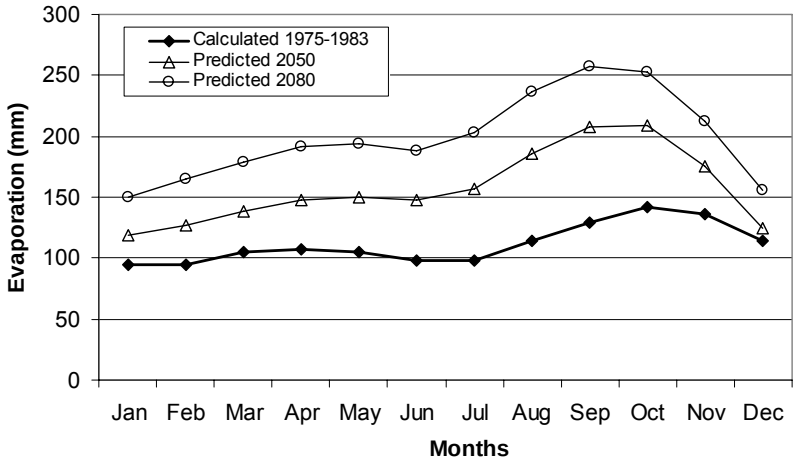

Figure 8: Estimated pan evaporation (1975-1983) in the Upper Suriname river basin and estimated future pan evaporation (GCM scenarios: 2050, 2080).

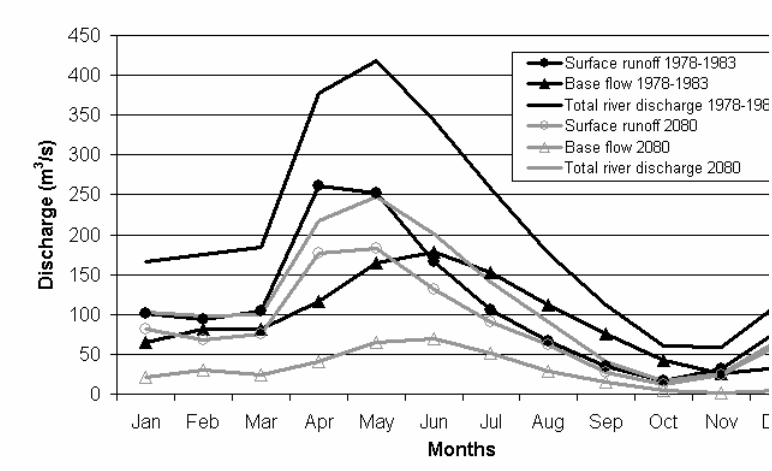

Figure 9: Mean monthly values of river discharge, surface runoff and base flow of the Upper Suriname river basin for the period 1978-1983 and the future period 2080 (GCM scenarios).

Climate change impact on the Upper Suriname river basin

Table 8a shows the annual water balance components for the 1978-1983 period and for the future periods 2050 and 2080 based on GCM results. The results indicate that for the GCM climate scenario year 2050, a 12% increase in mean annual precipitation and a 8% increase in mean annual evapotranspiration results in a reduction of the mean annual river discharge in the Upper Suriname river by 24% reference to the 1978-1983 period. From the obtained results, we can conclude that a small change in the mean annual temperature (1.8^{o}C and 3.2^{o}C for 2050 and 2080 respectively) has a significant impact on the river discharge. The annual river discharge components changes as follows: surface runoff decreases by 15% and base flow decreases by 40%. The monthly base flow and surface runoff reduction varies between 35% to 77% and 9% to 31% respectively. It is also found that for the GCM scenario year 2080, a decrease of 0.6% in mean annual precipitation and an increase in mean annual evapotranspiration of 17% results in a decrease of 35% in the mean annual river discharge. Surface runoff decreases by 19% and base flow decreases by 56%. The monthly base flow

and surface runoff reduction vary between 60% to 92% and 6% to 42% respectively. The decrease in river discharge can be explained by the fact that evaporation from the soil and transpiration from plants increases. The impact of climate change on the different runoff components of the Upper Suriname river basin for the GCM scenarios year 2080, simulated with the WetSpa model, is graphically presented in Fig. 9. From these plots we can also see that, during January-June (wet season), surface runoff is the main source of the total river discharge while during July-November (dry season) base flow is mainly contributing to the river discharge. This is also shown in Table 8b.

Table 8: (a) Annual water balance components for the current (1978-1983) and future periods (GCM scenarios for 2050, 2080), (b) change in mean monthly precipitation, total river discharge, surface runoff and base flow for future periods (GCM scenarios for 2050, 2080). The values in brackets are percentages referring to the 1978-1983 period. P is precipitation, Qt is total river discharge, Qs is surface runoff and Qb is base flow.

Component \ Period	**1978-1983**	**2050**	**2080**
Precipitation (mm)	14,052	15,734 (12%)	13,963 (-0.6%)
Actual evapotranspiration (mm)	8,528	9,171 (8%)	9,929 (17%)
Total river discharge (mm)	4,956	3,733 (-24%)	3,230 (-35%)
Surface runoff (mm)	2,667	2,269 (-15%)	2,169 (-19%)
Base flow (mm)	2,289	1,385 (-40%)	1001 (-56%)
Difference in soil and groundwater storage (mm)	568	2830	804

(a)

Period		**2050**				**2080**		
Component	**P (mm)**	**Qt (m^3/s)**	**Qs (m^3/s)**	**Qb (m^3/s)**	**P (mm)**	**Qt (m^3/s)**	**Qs (m^3/s)**	**Qb (m^3/s)**
Jan	-15.5 (9)	-60 (36)	-32 (31)	-28 (43)	-24.8 (15)	-63 (38)	-20 (20)	-43 (66)
Feb	-19.6	-64 (37)	-23 (24)	-41 (51)	-34.1 (22)	-77 (44)	-26 (28)	-51 (63)
Mar	(12)	-58 (32)	-17 (17)	-40 (49)	-27.9 (12)	-85 (46)	-28 (27)	-57 (70)
Apr	-15.5 (7)	-96 (25)	-51 (20)	-46 (40)	-43.4 (13)	-159 (42)	-84 (32)	-75 (65)
May	-27 (8)	-109 (26)	-51 (20)	-58 (35)	-24.8 (6)	-170 (41)	-70 (42)	-99 (60)
Jun	-31 (8)	-87 (25)	-22 (13)	-65 (37)	6.2 (2)	-142 (41)	-35 (21)	-108 (61)
Jul	3 (1)	-73 (28)	-9 (9)	-64 (42)	21.7 (9)	-117 (45)	-16 (15)	-102 (67)
Aug	12.4 (5)	-62 (35)	-6 (9)	-55 (49)	65.1 (43)	-86 (49)	-4 (6)	-83 (74)
Sep	37.2	-50 (45)	-5 (14)	-45 (59)	-18.6 (20)	-70 (63)	-9 (26)	-62 (82)
Oct	(24)	-34 (57)	-4 (24)	-30 (70)	-12.4 (22)	-43 (72)	-5 (29)	-38 (88)
Nov	-9 (10)	-27 (47)	-7 (22)	-20 (77)	0 (0)	-33 (57)	-9 (28)	-24 (92)
Dec	-9.3 (16)	-33 (29)	-12 (15)	-22 (65)	9.3 (5)	-47 (41)	-18 (24)	-29 (85)
	0 (0)							
	6.2 (3)							

(b)

Table 9 shows the changes in annual water balance components caused by hypothetical climate scenarios. The hypothetical scenarios shows that a 2°C and 4°C increase in temperature and no change in precipitation, causes a decrease in the total annual river discharge of 16% and 29.3% respectively. Surface runoff decreases by about 7.3% and 13.9% respectively and base flow decreases by about 30.1% and 50% respectively. The

results are quit close to the WetSpa simulations using the GCM predictions for 2050 (~ T+2°C) and 2080 (~ T+4°C) respectively (see Table 8a and 9). When precipitation is increased up till 50%, the WetSpa model simulates an increase in annual river discharge up till 75% and 57% for T+2°C and T+4°C respectively. Surface runoff and base flow also increases (see Table 9). The fact that the estimated river discharge for T+4°C is lower than for T+2°C may be caused by the higher evapotranspiration. When precipitation is decreased up till 50%, the annual river discharge decreases up till 84% and 87.5% for T+2°C and T+4°C respectively. Surface runoff and base flow also decreases. The difference in hydrologic simulation results may be caused by the amount of changes generated from the GCM results and hypothetical scenarios, and the calculation method of the future scenarios. Hypothetical scenarios are found to give a good view of how water balance components may change under different climate change conditions. GCM outputs however may give more realistic climate change results, because the outputs are based on climate modeling results using observed climatological data. Taking this into account and the limitations presented in paragraph 1, the values presented in Table 8 and 9 give only an order of magnitude of a response to a hypothetical change in temperature and precipitation due to climate change.

Table 9: Changes in annual water balance components in percentage for future periods caused by the following hypothetical scenarios (a) T+2°C P±10%, P±30%, P±50% and (b) T+4°C P±10%, P±30%, P±50%. The future values are given in percentages reference to the 1978-1983 period. T is the temperature and P is precipitation.

Component \ Period	**T+2°C, P-50%**	**T+2°C, P-30%**	**T+2°C, P-10%**	**T+2°C, P+0%**	**T+2°C, P+10%**	**T+2°C, P+30%**	**T+2°C, P+50%**
Actual evapotranspiration	-32	-13.2	2.4	9.3	16	27.8	38.6
Total river discharge	-84	-61.2	-32	-16	0.9	36.8	75
Surface runoff	-76.5	-53.4	-24	-7.3	11.4	54.7	104.1
Base flow	-93.1	-71.8	-44.1	-30.1	-16.1	9.7	33.5

(a)

Component \ Period	**T+4°C, P-50%**	**T+4°C, P-30%**	**T+4°C, P-10%**	**T+4°C, P+0%**	**T+4°C, P+10%**	**T+4°C, P+30%**	**T+4°C, P+50%**
Actual evapotranspiration	-29.9	-8.4	9.3	17	24.3	37.3	48.9
Total river discharge	-87.5	-69.3	-43.8	-29.3	-13.5	20.5	57
Surface runoff	-78.8	-57.1	-29.7	-13.9	3.9	44.9	92.1
Base flow	-97.8	-84.3	-62.4	-50.1	-37.5	-13.2	9.5

(b)

Both type of climate scenarios have shown that the Upper Suriname river basin is sensitive to climate change. Such large annual and monthly changes in the water balance may result in extreme events such as flooding and drought. The most dramatic case is for T+2°C (see Table 9). If the river discharge in the Upper Suriname river will decrease, this will also have significant impact on hydropower generation in the future. The decrease in surface runoff and base flow will also have its impact on the vegetation cover (tropical forest might change into dry forest) and in turn again affect the amount of water resources. If river discharges will increase, this will cause water levels to rise, resulting in flooding of the river banks and changes in the morphology of rivers. It should however be noticed that an increase in surface air temperature will not only affect precipitation and evapotranspiration, but factors such as solar radiation, wind, cloudiness and vegetation cover may also affect the basin hydrology.

Discussion and conclusions

This paper presents a spatial distributed hydrologic modeling and GIS approach for the assessment of climate change on the hydrological processes in a large tropical basin. The WetSpa model produced moderate simulation results for the river flows in the Upper Suriname river basin at daily time step, with parameters calibrated against measured river discharges series.

The hydrological simulation of the GCM scenario years 2050 and 2080 indicate that the annual river discharge in the Upper Suriname river basin will decrease in magnitude (maximum 35%). This decrease may change vegetation cover in time and in turn again affect the discharge in the Upper Suriname river. When applying hypothetical scenarios (T+2^{o}C, T+4^{o}C and P+10%, 30% and 50%), the WetSpa model simulates an increase in annual river discharges in the river basin of maximum 75%, and for T+2^{o}C, T+4^{o}C and P-10%, -30% and -50%, the river discharge is predicted to decrease with maximum 87.5%. The results obtained by both methods, do differ much from each other. Hypothetical climate change scenarios however give a better indication of how hydrological processes might change due to gradual changes in temperature.

The difference in simulated water balance components based on GCM and hypothetical scenarios may be explained by the application of the type of scenarios (e.g. uniform change in temperature in the case of hypothetical scenarios, limitations of GCM models). Therefore, the simulated runoff values in this study give only an order of magnitude of plausible changes. Uncertainties in the simulated future water balance components can also be caused be the model performance of the WetSpa model. This could be increased by using field parameters instead of literature values, longer historical data series for calibration and more hydrological observations (e.g. base flow) for calibration of the model. The uncertainty of river discharge prediction for hydrological modeling using climate change scenarios is also caused by the fact that precipitation patterns from a coarse gridded GCM are uncertain. Besides the many uncertainties in GCMs, the uncertainties in the climate scenarios may also cause deviations in the predictions (Giorgi et al, 2001; Mearns et al, 2003). It is therefore advised to use downscaling techniques and regional climate models (RCMs) in future studies (Menzel and Burger, 2002). Regional scenarios of future climate can be used to study the “true” impacts of climate change on the river discharge in the Upper Suriname river basin. Another uncertainty in the obtained results is the lack of knowledge about the future change in evapotranspiration. As less is known about the ability of the WetSpa model to simulate future changes in water balance components under climate change conditions, it would also be useful to apply more hydrological models to this study area for the same purpose. Future work on the impact of climate change should also be extended by the consideration of changes in land cover due to the interaction between climate change and changes in vegetation composition. This study shows that the estimated changes in runoff are large enough to be considered for future impact analyses e.g. flood studies, effect on hydropower generation.

Acknowledgements

This research is financially supported by the Research and Development Fund of the University of Suriname under project No. Bv/FB/sw-520. Sincere thanks to Dr. Y. B. Liu (Vrije Universiteit Brussel, Belgium) for the provision of the WetSpa model, and the National Center for Atmospheric Research (NCAR- USA) for the provision of the MAGICC/SCENGEN model 4.1. We are also grateful to three anonymous reviewers for a number of valuable review comments.

REFERENCES

Ambrizzi, T., de Souza, E. B., Pulwarty, R. S. (2005). The Hadley and Walker regional circulations and associated ENSO impacts on South American seasonal rainfall, In: H. F. Diaz, R. S. Bradley (Editors), The Hadley Circulation: present, past and future. Kluwer Academic Publishers, Netherlands, pp. 203-231.

Andersen, J., Refsgaard, J.C., Jensen, K.H. (2001). Distributed hydrological modeling of the Senegal River Basin – model construction and validation. Journal of Hydrology, 247, pp. 200-214.

Arnold, J.G., Srinivasan, R., Muttiah, R.S., Willieam, J.R. (1998). Large area hydrological modeling and assessment, Part I: Model development. J. Am. Water Resour. Ass. 34 (1). pp. 73-89.

Bergstrom, S., Forsman, A. (1973). Development of a conceptual deterministic rainfall-runoff model. Nord Hydrol. 4, pp. 147-170.

Beven, K. (1989). Changing ideas in hydrology – the case of physically based models. Journal of Hydrology 105, pp. 157-172.

Beven, K. J. (2000). Precipitation-runoff modeling. John Willey and Sons Ltd, England.

Beven, K. J., Kirkby, M.J. (1979). A physical based variable contributing area model of basin hydrology. Hydrol. Sci. Bull 24 (1). pp. 43-69.

Booij, M.J. (2002). Appropriate modeling of climate change impacts of river flooding. PhD. Thesis, Universiteit Twente, Nederland.

Booij, M.J. (2005). Impact of climate change on river flooding assessed with different spatial model resolutions. Journal of Hydrology, 303, pp. 176-198.

Boorman, D.B., Sefton, C.E.M. (1997). Recognizing the uncertainties in the quantification of the effects of climate change on hydrological response. Climate Change, 35, pp. 415-434.

Bormann, H. (2005). Regional hydrological modeling in Benin (West Africa): Uncertainty issues versus scenarios of expected future environmental change. Physics and Chemistry of the Earth, 30, pp. 472-484.

Bronstert, A.Niehoff, D., Burger, G. (2002). Effects of climate and land use change on storm runoff generation: present knowledge and modeling capabilities. Hydrol. Process. 16, pp. 209-529.

Brooks, R.H., Corey, A.T. (1966). Properties of porous media affecting fluid flow, J. Irrig. Drain. Amer. Soc. Civil. Eng. IR2, pp. 61-88.

Calver, A., Wood, W.L. (1995). Chapter 17: The institute for hydrology distributed model, In: Computer model of watershed hydrology, V.P. Singh (ed), Water Resources Publications, Littleton, Colo.

Campling, P., Gobin, Q., Beven, K., Feyen, J. (2002). Rainfall-runoff modeling of a humid tropical catchment: the TOPMODEL approach. Hydrological Processes, 16, pp. 231-253.

Crawford, N.H., Linsley, R.K. (1966). Digital simulation in hydrology-Stanford watershed model IV. Tech.Rep. 39, Standford University, Standford.

Eagleson, P.S. (1978). Climate, soil, and vegetation, a simplified model of soil moisture movement in liquid phase, Water Resour. Res. 14(5), pp. 722-730.

Gellens, D., Roulin, E. (1998). Stream flow response of Belgian catchments to IPCC climate change scenarios. Journal of Hydrology, 210, pp. 242-258.

Gianninni, A., Kushnir, Y., Cane, M. (2000). Interannual variability of Caribbean rainfall, ENSO and the Atlantic Ocean, Journal of Climate 13, pp. 297-311.

Giorgi, F., Hewitson, B., Christensen, J., Hulme, M., Von Storch, H., Whetton, P., Jones, R., Mearns, L., Fu, C. (2001). Regional Climate Information: Evaluation and Projections (chapter 10). In: J.Houghton et al (Editors), Climate Change 2001: The Scientific

Basis, Contribution of Working I to the Third Assessment Report of the IPCC, Cambridge U. Press, pp. 585-629.

Glen, B. (2004). Introduction to climate change, Inc, http://www.climateark.org/vital/intro.asp (assessed July 16, 2004)

Gleick, P.H. (1986). Methods for evaluating the regional hydrological impacts of global climatic changes. Journal of Hydrology, 88, pp. 97-116.

Guex, F. (2001). Modelisation hydrologique dans le basin versant de l'Alzette (Luxembourg), regionalization des parameters d'un modele global, Travail pratique de Diplome, Ecole Polytecnique Federale de Laussanne 67.

Houben, L., Molenaar, A. (undated). Rehabilitation of the East-West Road Connection, causes and repair methods of road cracks in recently rehabilitated road stretch and advice on technical specifications for a planned new road (draft). Delft University of Technology, the Netherlands.

Hulme, M., Wigley, T.M.L., Barrow, E.M., Raper, S.C.B., Centella, A., Smith, S.J., Chipanshi, A.C. (2000). Using a Climate Scenario Generator for Vulnerability and Adaptation Assessments: MAGICC and SCENGEN Version 2.4. Workbook, Climatic Research Unit, Norwich UK.

IPCC (2001). Climate change 2001: The Scientific Basis. Contribution of Working Group I to the Third Assessment Report of the Intergovernmental Panel on Climate Change (Watson, R., Houghton, J., Ding, Y., Griggs, J., Noguer, M., van der Linden, P., Dai, X. Maskell, K., Johnson, C. (Editors), Cambridge University Press, United Kingdom.

IPCC-TGCIA (1999). Guidelines on the Use of Scenario Data for Climate Impact and Adaptation Assessment. Version 1. Prepared by Carter, T.R., M. Hulme, M. Lal, Intergovernmental Panel on Climate Change, Task Group on Scenarios for Climate Impact Assessment. Technical report.

Legesse, D., Vallet-Coulomb, C., Gasse, F. (2003). Hydrological response of a catchment to climate and land use changes in Tropical Africa: a case study South Central Ethiopia, Journal of Hydrology, 275, pp. 67-85.

Lenselink, K., van der Weert, R. (1970). Estimating free water evaporation in Suriname, Surinaamse Landbouw, Suriname.

Leavesley, G.H., Lichty, R.W., Troutman, B.M., Saindon, L.G. (1983). Precipitation-runoff modeling system. User manual. USGS waterresources investigation report 83-4238, USGS, Denver.

Lindstrom, G., Johansson, B., Persson, M. Gardelin, M. and Bergstrom, S. (1997). Development and test of the distributed HBV-96 hydrological model. J. Hydrol. 201, pp. 272-288.

Liu, Y. (1999). GIS-based spatially distributed hydrological modeling of the Barebeek catchment. M.Sc. Thesis, Vrije Universiteit Brussel, Belgium.

Liu, Y.B., De Smedt, F. (2004). WetSpa extension, a GIS based hydrologic model for flood prediction and watershed management. Technical report, Vrije Universiteit Brussel, Belgium.

Liu, Y. (2004). Development and application of a GIS based hydrological model for flood prediction and watershed management. Ph.D. Thesis, Vrije Universiteit Brussel, Belgium.

Maidment, D. (1992). Handbook of Hydrology. McGrawHill Inc, United States of America.

Martis, A., van Oldenburg, G.J., Burgers, G. (2002). Predicting rainfall in the Dutch Caribbean – more than El Nino?, Int. J. Climatol. 22, pp. 1219-1234.

Marshall, J., Kushnir, Y., Battisti, D., Change, P., Czaja, A., Dickson, R., Hurrel, J., McCartney, M., Saravanan, R., Visbeck, M. (2001). North Atlantic Climate Variability: phenomena, impacts and mechanism, Int. J. Climatol, 21, pp. 1863-1898.

Mearns, L.O., Giorgi, F., Whetton, P., Pabon, D., Hulme, M., Lal, M. (2003). Guidelines for use of climate scenarios developed from regional climate model experiments, DDC of IPCC TGCIA (final version), pp. 1-38.

Menzel, L., Burger, G. (2002). Climate change scenarios and runoff response in the Mulde catchment (Southern Elbe, Germany). Journal of Hydrology, 267, pp. 53-64.

Miller, W.A., Cunge, J.A. (1975). Simplified equations of unsteady flow, In: Unsteady flow in open channels, Mahmood, K. and Yevjevich, V. (ed). Water Resources Publications, Fort Collins, CO.

Mol, J., Resida, D., Ramlal, J., Becker, C. (2000). Effects of El Niño-related drought on freshwater and brackish water fishes in Suriname, South America, Environmental Biology of Fishes 59, pp. 429-440.

Molicova, H., Grimaldi, M. Bonell, M., Hubert, P. (1997). Using top model towards identifying and modeling the hydrological patterns within a headwater, humid, tropical catchment. Hydrological Processes, 11, pp. 1169-1196.

Nash, J.E., Sutcliffe, J.V. (1970). River flow forecasting through conceptual model, J.Hydrol. 10, pp. 282-290.

Niemanm J., Strzepek, K., Yates, D. (1994). Impacts of spatial and temporal data on a climate change assessment of Blue river Nile, WP 94-44, IIASA, Laxenburg, Austria.

Nurmohamed, R., Naipal, S. (2004). Trends and Variation in Monthly Precipitation and Temperature in Suriname, Final Proc. Int. Conf. BALWOIS Conference on Water Observation and Information System for Decision Support. Ohrid, FY Republic of Macedonia, pp. 3.

Perrin, C., Michel, C., Andreassian, V. (2001). Does a large number of parameters enhance model performance? Comparative assessment of common catchment model structures on 429 catchments. Journal of Hydrology, 242, pp. 275-301.

Rajagopolan, B., Kushir, Y., Tourre, Y., Cane, M. (1997). Temporal Variability of North Atlantic Oscillation and Tropical Atlantic SST, Lamont-Doherty Earth Observatory of Columbia University, New York, http://www.aoml.noaa.gov/Phod/acvp/raja.htm (assessed November 25, 2005)

Refsgaard, J. C., Storm, B. (1995). Chapter 23 MIKE SHE, In: Computer model of Watershed hydrology, V.P. Singh (ed), Water Resources Publ., Littleton, Colo.

Robock, A., Turco, R.P., Harwell, M.A., Ackerman, T.P., Andressen, R., Chang, H.S., Sivakumar, V.K. (1993). Use of general circulation model output in the creation of climate change scenarios for impact analyses, Climate Change 23, pp. 293-335.

Seifu, G. (2003). Modeling the effect of climate and land-use changes on the hydrological processes: an integrated GIS and distributed modeling approach. Ph.D. Thesis, Vrije Universiteit Brussel, Belgium.

Verhoog, F. (1987). Impact of climate change on the morphology of river basins, In: Solomon, S., Beram, M. et al The influence of climate change and climate variability on the hydrological regime and water resources, IAHS publ. 168, Washington, USA, pp.315-326.

Wang, C., (2001). Atlantic climate variability and its associated atmospheric circulation cells, Int. J. of Climate, 15, pp. 1516-1536.

Wang, C., (2005). ENSO, Atlantic climate variability, and the Walker and Hadley circulations, In: H.F. Diaz, H.F, R.S. Bradley, R.S. (Editors). The Hadley Circulation: present, past and future, Kluwer Academic Publishers, Netherlands, pp. 173-202.

Wigley, T., (2003). MAGICC/SCENGEN 4.1 Software and manual, NCAR, Boulder, CO, USA.

Wittenberg, H., Sivapalan, M. (1999). Watershed groundwater balance estimation using stream flow recession analysis and base flow separation, J. Hydrol 219, pp. 20-33.

USACE (1998). HEC-1 Flood Hydrograph Package: user's manual, US Army Corps of Engineers, Davis, CA.